Periodica Polytechnica
Mechanical Engineering

Operation of Looped District Heating Networks

61(2), pp. 79-86, 2017
https://doi.org/10.3311/PPme.9256

László Garbai[1], Andor Jasper[1*]

RESEARCH ARTICLE

Received 30 March 2016; accepted after revision 02 September 2016

Abstract

The study presents a methodology for the optimal operation of district heating networks with a circular conduit system. The authors discuss this this topic in an absolutely general form. By a special statement and solution of Kirchhoff Laws, node equations and loop equations, the hydraulic end point of the circle is determined, including the supply ratio of the consumer located at the hydraulic end point. Two objective functions are stated by the authors; one of them for the minimum of flow work, and the other for the minimum of power supplied. It is demonstrated that the objective functions yield different results. Theoretically more economical operation is ensured by the flow pattern resulting from the minimization of the power supplied.

Keywords

looped district heating network, dissipated energy, minimum of energy input, hydraulic analysis, minimum of dissipated energy

[1] Department of Building Service and Process Engineering,
Faculty of Mechanical Engineering,
Budapest University of Technology and Economics,
H-1111 Budapest, Bertalan Lajos utca 4-6., Hungary

[*] Corresponding author, e-mail: jasper@epgep.bme.hu

1 Introduction

As regards energetics in Europe, district heating plays a prominent role in the heat supply of large cities. District heating systems have extensive conduit networks. The hydraulic examination of conduit networks, adjustment of a hydraulic optimum, of the optimal pump operating point represent key issues in network operation. Some part of conduit networks is radial, another part is of loop topography. The operation of loop networks is more complicated; the flow pattern produced is generally unstable due to changes in consumer demands in Ref. [2-4]. The method of Krope et al. is based on nonlinear optimization in Ref. [5-8]. In Ref. [9] the optimal operation is based on fast fluid-dynamic simulation. In Ref. [10] a fluid dynamic model of the network based on conservation was built and a genetic algorithm used in order to minimize the energy required by the system. A technical-economical optimization with the aim of minimizing both the pumping energy consumption and the thermal energy losses while maximizing the yearly annual revenue is performed in Ref. [11]. A method for district heating network dimensioning, based on the probabilistic determination of the flow rate for hot water heating was carried out in Ref. [12]. In Ref. [13] a multi-objective optimization model is performed for the best network design considering both initial investment for pipes and pumping cost for water distribution. In our research, methods for the hydraulic analysis of loop and radial networks were examined. It is a widely held view that loop networks are hydraulically more advantageous than radial networks. In the course of our research, the explicitness of this theorem was disproved. This study presents only the part of our research discussing a hydraulic analysis method for district heating networks containing one loop. Objective functions are stated for this type of network and the flow pattern is determined by minimizing the objective function. One of the objective functions states the minimization of flow work. The other objective function aims for the minimum of power supplied. The flow patterns yielded by the solution of the two objective functions differ from each other. Our study discusses the solution of both objective functions.

2 Objective functions and hydraulic equations

Figure 1 shows the topological model (graph) of the pipeline system of a district heating network with a circular conduit system. Consumer hot water flow demands are given and known: $\dot{V}_0,\dot{V}_1,\dot{V}_2,\ldots\dot{V}_n,\dot{V}_0^*,\dot{V}_1^*,\dot{V}_2^*,\ldots\dot{V}_n^*$. An optimal flow pattern is sought for, with a minimum dissipated energy and / or energy input or pump work. Thus, the problem is examined by solving two objective functions, using two models.

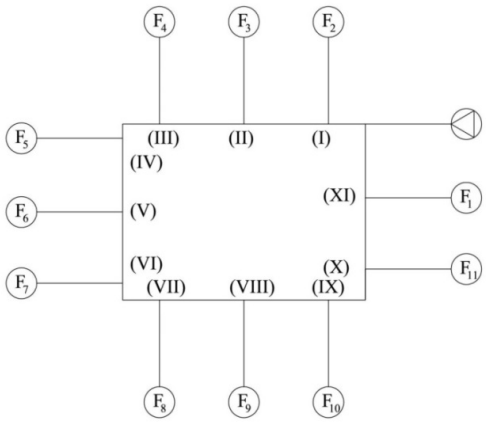

Fig. 1 Topological model graph of a district heating network with a circular conduit system

In the first task, the objective function is to determine the dissipated energy minimum. This is equivalent to the flow pattern yielded by the solution of Kirchhoff Laws [1].

In the second task, Kirchhoff Law II is allowed to be infringed by placing two pumps at the input point – with right and left side feed. Then the aggregate figures of differential pressures on the right and left side branches are not necessarily equal. The pump works yielded in the two solutions are compared and their differences are evaluated. The network is opened up at the feed point in both models. Figure 2 shows the topology pattern and flow.

2.1 Flow pattern at the minimization of dissipated energy [1]

The problem is presented on the network of Fig. 2 by depicting the network of Fig. 1 in a general format, for an n number of consumers.

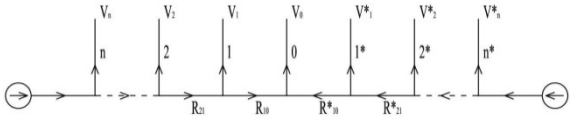

Fig. 2 District heating network with opened circular conduit

The flow pattern can be sought for by solving the loop equation. In our assumption, the hydraulic end point in the flow is (0), from whose demand is supplied through branch n-0 and through branch 0-n*. Thus, the unknown quantity is proportional factor k.

The objective function:

$$\sum_{i=1}^{n} R_i \dot{V}_i^3 \rightarrow min! \tag{1}$$

Conditional equations:

a) node equation:

$$\sum_{j=1}^{n} \dot{V}_{i,j} = 0 \forall i \tag{2}$$

where

i – is the number of nodes,

j – is the index of branches connected to node i.

b) loop equation:

$$\begin{aligned} & R_{10}\left(k\dot{V}_0\right)^2 + R_{21}\left(k\dot{V}_0 + \dot{V}_1\right)^2 + \cdots \\ & + R_{n,n-1}\left(k\dot{V}_0 + \dot{V}_1 + \dot{V}_2 + \cdots + \dot{V}_{n-1}\right)^2 \\ & + R_{n+1}\left(k\dot{V}_0 + \dot{V}_1 + \dot{V}_2 + \cdots + \dot{V}_n\right)^2 \\ & = R_{10}^*\left((1-k)\dot{V}_0\right)^2 + R_{21}^*\left((1-k)\dot{V}_0 + \dot{V}_1^*\right)^2 \\ & + \cdots + R_{n+1}^*\left((1-k)\dot{V}_0 + \dot{V}_1^* + \dot{V}_2^* + \cdots \dot{V}_n^*\right)^2 \end{aligned} \tag{3}$$

A quadratic equation is yielded for k by rearrangement of the loop equation.

$$\begin{aligned} & \left(R_{10} + R_{21} + \cdots + R_{n+1}\right)\left(k\dot{V}_0\right)^2 + 2\Big[kR_{21}\dot{V}_0\dot{V}_1 + kR_{32}\dot{V}_0 \\ & \left(\dot{V}_1 + \dot{V}_2\right) + \cdots + kR_{n+1}\dot{V}_0\left(\dot{V}_1 + \dot{V}_2 + \cdots + \dot{V}_n\right)\Big] \\ & + R_{21}\dot{V}_1^2 + R_{32}\left(\dot{V}_1 + \dot{V}_2\right)^2 + \cdots + R_{n+1}\left(\dot{V}_1 + \dot{V}_2 + \cdots + \dot{V}_n\right)^2 \\ & = \left(R_{10}^* + R_{21}^* + \cdots + R_{n+1}^*\right)\left((1-k)\dot{V}_0\right)^2 \\ & + 2\Big[R_{21}^*(1-k)\dot{V}_0\dot{V}_1^* + (1-k)R_{32}^*\dot{V}_0\left(\dot{V}_1^* + \dot{V}_2^*\right) \\ & + \cdots + (1-k)R_{n+1}^*\dot{V}_0\left(\dot{V}_1^* + \dot{V}_2^* + \cdots + \dot{V}_n^*\right)\Big] \\ & + R_{21}^*\dot{V}_1^{*2} + R_{32}^*\left(\dot{V}_1^* + \dot{V}_2^*\right)^2 + \cdots + R_{n+1}^*\left(\dot{V}_1^* + \dot{V}_2^* + \cdots + \dot{V}_n^*\right)^2. \end{aligned} \tag{4}$$

By further rearrangement:

$$\begin{aligned} & k^2 \cdot \left(R_{10} + R_{21} + \cdots + R_{n+1}\right) \cdot \dot{V}_0^2 + 2k \cdot \\ & \left[R_{21} \cdot \dot{V}_0 \cdot \dot{V}_1 + R_{32} \cdot \dot{V}_0 \cdot \left(\dot{V}_1 + \dot{V}_2\right) + \cdots + R_{n+1} \cdot \dot{V}_0 \cdot \left(\dot{V}_1 + \dot{V}_2 + \cdots + \dot{V}_n\right)\right] \\ & + \left[R_{21} \cdot \dot{V}_1^2 + R_{32} \cdot \left(\dot{V}_1 + \dot{V}_2\right)^2 + \cdots + R_{n+1} \cdot \left(\dot{V}_1 + \dot{V}_2 + \cdots + \dot{V}_n\right)^2\right] \\ & = \left(1-k\right)^2 \cdot \left(R_{10}^* + R_{21}^* + \cdots + R_{n+1}^*\right) \cdot \dot{V}_0^2 \\ & + 2\left(1-k\right)\left[R_{21}^* \cdot \dot{V}_0 \cdot \dot{V}_1^* + \cdots + R_{n+1}^* \cdot \dot{V}_0 \cdot \left(\dot{V}_1^* + \dot{V}_2^* + \cdots + \dot{V}_n^*\right)\right] \\ & + \left[R_{21}^* \cdot \dot{V}_1^2 + R_{32} \cdot \left(\dot{V}_1^* + \dot{V}_2^*\right)^2 + \cdots + R_{n+1} \cdot \left(\dot{V}_1^* + \dot{V}_2^* + \cdots + \dot{V}_n^*\right)^2\right]. \end{aligned} \tag{5}$$

Signs introduced:

$$A=\left(R_{10}+R_{21}+\cdots+R_{n+1}\right),$$
$$B=\left[R_{21}\dot{V}_0\dot{V}_1+R_{32}\dot{V}_0\left(\dot{V}_1+\dot{V}_2\right)+\cdots+R_{n+1}\dot{V}_0\left(\dot{V}_1+\dot{V}_2+\cdots+\dot{V}_n\right)\right],$$
$$C=\left[R_{21}\cdot\dot{V}_1^2+R_{32}\cdot\left(\dot{V}_1+\dot{V}_2\right)^2+\cdots+R_{n+1}\cdot\left(\dot{V}_1+\dot{V}_2+\cdots+\dot{V}_n\right)^2\right],$$
$$A^*=\left(R_{10}^*+R_{21}^*+\cdots+R_{n+1}^*\right),$$
$$B^*=\left[R_{21}^*\cdot\dot{V}_0\cdot\dot{V}_1^*+R_{32}^*\cdot\dot{V}_0\cdot\left(\dot{V}_1^*+\dot{V}_2^*\right)+\cdots+R_{n+1}^*\cdot\dot{V}_0\cdot\left(\dot{V}_1^*+\dot{V}_2^*+\cdots+\dot{V}_n^*\right)\right],$$
$$C^*=\left[R_{21}^*\cdot\dot{V}_1^{*2}+R_{32}\cdot\left(\dot{V}_1^*+\dot{V}_2^*\right)^2+\cdots+R_{n+1}\cdot\left(\dot{V}_1^*+\dot{V}_2^*+\cdots+\dot{V}_n^*\right)^2\right].$$

Constants stated in a closed form:

$$\begin{aligned}
A&=\sum\nolimits_{j=0}^{n}R_{j(j+1)},\\
B&=\left[\sum\nolimits_{j=0}^{n-1}\left(R_{(j+1)(j+2)}\cdot\sum\nolimits_{i=1}^{i+j}\dot{V}_i\right)\right]\cdot\dot{V},\\
C&=\sum\nolimits_{j=0}^{n-1}\left[R_{(j+1)(j+2)}\cdot\left(\sum\nolimits_{i=1}^{i+j}\dot{V}_i\right)^2\right],\\
A^*&=\sum\nolimits_{j=0}^{n^*}R_{j(j+1)}^*,\\
B^*&=\left[\sum\nolimits_{j=0}^{n^*-1}\left(R_{(j+1)(j+2)}^*\cdot\sum\nolimits_{i=1}^{i+j}\dot{V}_i^*\right)\right]\cdot\dot{V}_0,\\
C^*&=\sum\nolimits_{j=0}^{n^*-1}\left[R_{(j+1)(j+2)}^*\cdot\left(\sum\nolimits_{i=1}^{i+j}\dot{V}_i^*\right)^2\right].
\end{aligned}\tag{6}$$

Quadratic equation using the signs:

$$k^2A\dot{V}_0^2+2kB+C=\left(1-k\right)^2A^*\dot{V}_0^2+2\left(1-k\right)B^*+C^*\tag{7}$$

After rearrangement:

$$k^2\left(A-A^*\right)\dot{V}_0^2+2k\left(B+A^*\dot{V}_0^2+B^*\right)+\left(C-C^*-A^*\dot{V}_0^2-2B^*\right)\tag{8}$$

The equation yields two solutions for proportional factor k; for the most part, only one of them has real physical content, this latter yielding flows $\dot{V}_{01}$ and $\dot{V}_{01}^*$ and finally, flows $\dot{V}_n$ and $\dot{V}_n^*$. In view of these flows, pressure losses on conduit sections can be calculated and the pressure pattern of the network can be set up, simultaneously yielding feed differential pressure and pump delivery head figures. Application of the loop rule also results in the fact that the aggregate of pressure loss figures is equal along routes 0-n and 0-n* , and pumps operate at identical delivery heads.

2.2 Flow pattern in the minimization of input power. Separated pumping at the feed location

Let us examine if the quantity of power supplied can be decreased by separated pumping, by opening the loop at the location of pumping.

Objective function to express the minimum of pumping work:

$$C=\left(\sum\dot{V}+k\cdot\dot{V}_0\right)\cdot\sum\Delta p+\left(\sum\dot{V}^*+\left(1-k\right)\cdot\dot{V}_0\right)\cdot\sum\Delta p^*\rightarrow min!\tag{9}$$

This objective function is of different structure compared to the function to express the search for minimum dissipated energy.

The minimum is placed where $\frac{d}{dk}C=0$, and

$$\begin{aligned}
\frac{dC}{dk}&=\dot{V}_0\cdot\sum\Delta p+\left(\sum\dot{V}+k\cdot\dot{V}_0\right)\cdot\frac{d}{dk}\sum\Delta p-\dot{V}_0\cdot\sum\Delta p^*\\
&+\left(\sum\dot{V}^*+\left(1-k\right)\cdot\dot{V}_0\right)\cdot\frac{d}{dk}\sum\Delta p^*=0.
\end{aligned}\tag{10}$$

Where, using the earlier signs,

$$\begin{aligned}
\sum\Delta p&=k^2\cdot A\cdot\dot{V}_0^2+2k\cdot B+C.\\
\frac{d}{dk}\sum\Delta p&=2k\cdot A\cdot\dot{V}_0^2+2\cdot B.\\
\sum\Delta p^*&=\left(1-k\right)^2\cdot A^*\cdot\dot{V}_0^2+2\left(1-k\right)\cdot B^*+C^*.\\
\frac{d}{dk}\sum\Delta p^*&=2k\cdot A^*\cdot\dot{V}_0^2-2\cdot A^*\cdot\dot{V}_0^2-2\cdot B^*.
\end{aligned}\tag{11}$$

Equation (8) with the signs introduced:

$$\begin{aligned}
&\dot{V}_0\cdot\left(k^2\cdot A\cdot\dot{V}_0^2+2k\cdot B+C\right)+\left(\sum\dot{V}+k\cdot\dot{V}_0\right)\cdot\left(2k\cdot A\cdot\dot{V}_0^2+2\cdot B\right)\\
&-\dot{V}_0\cdot\left(\left(1-k\right)^2\cdot A^*\cdot\dot{V}_0^2+2\left(1-k\right)\cdot B^*+C^*\right)\\
&+\left(\sum\dot{V}^*+\left(1-k\right)\cdot\dot{V}_0\right)\cdot\left(2k\cdot A^*\cdot\dot{V}_0^2-2\cdot A^*\cdot\dot{V}_0^2-2\cdot B^*\right)=0
\end{aligned}\tag{12}$$

After rearrangement, a quadratic equation is yielded for k:

$$\begin{aligned}
&k^2\cdot\left(A-A^*\right)3\cdot\dot{V}_0^3+k\cdot\left[2A\cdot\dot{V}_0^2\cdot\sum\dot{V}+4B\cdot\dot{V}_0\right.\\
&\left.+A^*\left(2\cdot\dot{V}_0^2\cdot\sum\dot{V}^*+6\cdot\dot{V}_0^3\right)+4B^*\cdot\dot{V}_0\right]\\
&+\left[2B\sum\dot{V}+C\cdot\dot{V}_0-A^*\left(3\cdot\dot{V}_0^3+2\cdot\dot{V}_0^2\sum\dot{V}^*\right)\right.\\
&\left.-B^*\cdot\left(4\cdot\dot{V}_0+2\sum\dot{V}^*\right)-C^*\cdot\dot{V}_0\right]=0.
\end{aligned}\tag{13}$$

The factor k expressing the division ratio of volumetric flow $\dot{V}_0$ can be determined by the root formula.

It can be observed that the expression to determine proportional factor k is not identical with expression (8), therefore results are also different. It is important to decide whether it is economical to invest in two pumps, that is, whether operating cost savings represent real yields in view of investment costs.

3 Example

Let us perform the hydraulic analysis of the looped district heating network shown in Fig. 3. Let us define the hydraulic end point of the network. Let us open the loop network into a radial network with two feed points. Our example presents calculations for the minimization of both dissipation energy and feed outputs.

3.1 Determination of the flow pattern with the minimum of energy dissipation

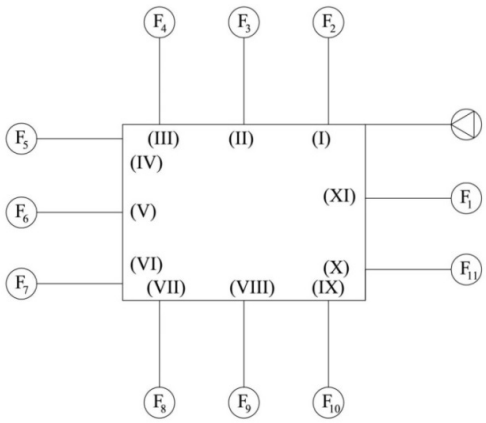

Fig. 3 Model of loop district heating network for calculations to minimize dissipation energy

Figure 4 illustrates the transformation of the network shown in Fig. 3 into a radial network with two input points.

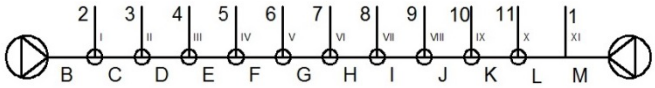

Fig. 4 Opened loop

Figure 4 shows the location of the 11 consumers along the mains conduit with two input points yielded after cutting the loop. The data required for performing the hydraulic analysis – name of section, length of section, caloric output, mass flow and standard pipe diameter – are shown in Table 1. Starting from the presumed end point towards the two inputs produced by cutting, end point consumer demand is supplied in a proportion $k\dot{V}_0$ from one direction, and in a proportion $(1-k)\dot{V}_0$ from the opposing direction. The presumed hydraulic end point is consumer 5. For reasons of expanse, results for consumers 4 and 6 as presumed hydraulic end points are not included herein. They represent figures higher than one and lower than zero, respectively, as expected.

Select consumer caloric center 5 as a hydraulic end point.

$$\dot{V}_5 = \dot{V}_0 = 0.0117\left[\frac{m^3}{s}\right]$$

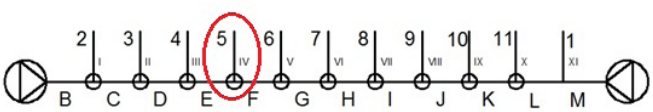

Fig. 5 Illustration of the presumed hydraulic end point

Table 1 Hydraulic data of each section

		L	$\dot{Q}$	$\dot{m}$	D
		m	*kW*	*kg/s*	*mm*
SECTIONS	B	1018	7454	58.79	200
	C	552	5894	46.48	150
	D	194	3494	27.56	150
	E	562	1934	15.25	150
	F	154	504	3.98	125
	G	468	64	0.51	80
	H	112	466	3.67	80
	I	160	906	7.14	100
	J	336	1606	12.67	200
	K	162	11446	90.27	250
	L	240	20596	162.43	250
	M	32	21426	168.97	250
CONSUMERS	1	324	830	6.55	100
	2	790	1560	12.30	100
	3	36	2400	18.93	125
	4	50	1560	12.30	100
	5	250	1430	11.28	80
	6	42	440	3.47	65
	7	94	530	4.18	65
	8	38	440	3.47	65
	9	220	700	5.52	65
	10		*9840*	77.60	
	11		*9150*	72.16	

By substituting the constants yielded in the quadratic correlation as described:

$$k^2\left(A-A^*\right)\dot{V}_0^2 + 2k\left(B + A^*\dot{V}_0^2 + B^*\right) + \left(C - C^* - A^*\dot{V}_0^2 - 2B^*\right)$$

Constant values:
$A = 3211.2380$,
$B = 0.7401$,
$C = 2.2177$,
$A^* = 36642.7233$,
$B^* = 2.2222$,
$C^* = 2.5400$.

So the factor after solution will be $k = 0.7937$ [-].

This result already corresponds to the expected solution; however, it cannot be stated clearly that this should be the end point of the system before verification thereof by calculations performed for further points.

Table 2 shows pressure values at each node and at the feed point. It can be observed that the feed pressure figures required, as calculated in the two directions, are in agreement.

Table 2 Pressure figures of nodes and feed points

	Δp [bar]		Δp [bar]
IV.	1.9202	IV.	1.9202
III.	2.0257	V.	1.9257
II.	2.2233	VI.	2.8904
I.	4.2035	VII.	3.5651
SZ1	5.5920	VIII.	4.1081
		IX.	4.1702
		X.	4.4022
		XI.	5.4424
		SZ2	5.5920

It can be observed that the aggregate of the differential pressure figures calculated from the two directions – that is, pump delivery head figures – agree. $\Delta p_{sz} = 5.5920$ bar.

The figures of volumetric flow delivered by the pumps correspond to the volumetric flow figures of sections B and M, respectively. $\dot{V}_{SZ1} = \dot{V}_B = 0.0547 \frac{m^3}{s}$, $\dot{V}_{SZ2} = \dot{V}_M = 0.1826 \frac{m^3}{s}$.

The power absorbed by each pump:

$P_1 = p_{SZ} \cdot \dot{V}_{SZ1} = 5.5920 \cdot 0.0547 = 0.3057 bar \frac{m^3}{s} = 30.57 kW$,

$P_2 = p_{SZ} \cdot \dot{V}_{SZ2} = 5.5920 \cdot 0.1826 = 1.021 bar \frac{m^3}{s} = 102.1 kW$.

The total power absorbed:

$P_{total} = P_1 + P_2 = 30.57 + 102.1 = 132.67 kW$.

The pressure pattern developed in the network is shown in Fig. 6.

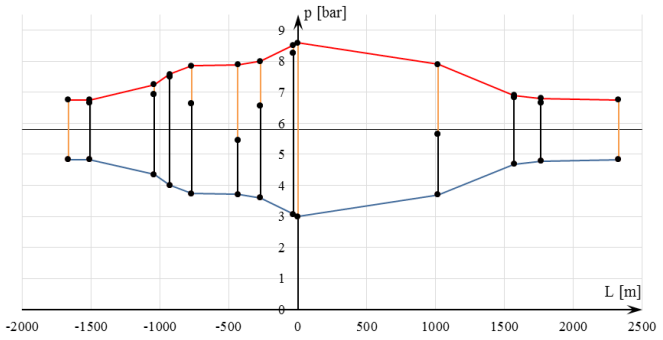

Fig. 6 Illustration of the presumed hydraulic end point

A pressure of at least 3 bar must be ensured at pump intake in order to avoid cavitation. Node pressures were modified accordingly. The red line shows pressure in the forward conduit, and the blue line indicates pressure in the return conduit. Green lines represent pressure drops in consumer branches, and black lines are dampers in consumer branches, required to reach the design pressure at each node.

3.2 Determination of the flow pattern with the minimum of energy input

The calculation principle of the basic data (heat power, mass flow, volumetric flow) coincides with the one presented for flow work minimization. In the calculation based on minimum energy input, the hydraulic end point came to be consumer 7. The data used in the calculation are shown in Table 3.

Table 3 Hydraulic data of each section

		L	$\dot{Q}$	$\dot{m}$	D
		m	kW	kg/s	mm
SECTIONS	B	1018	7454	58.79	200
	C	552	5894	46.48	150
	D	194	3494	27.56	150
	E	562	1934	15.25	150
	F	154	504	3.98	125
	G	468	64	0.51	80
	H	112	466	3.67	80
	I	160	906	7.14	100
	J	336	1606	12.67	200
	K	162	11446	90.27	250
	L	240	20596	162.43	250
	M	32	21426	168.97	250
CONSUMERS	1	324	830	6.55	100
	2	790	1560	12.30	100
	3	36	2400	18.93	125
	4	50	1560	12.30	100
	5	250	1430	11.28	80
	6	42	440	3.47	65
	7	94	530	4.18	65
	8	38	440	3.47	65
	9	220	700	5.52	65
	10		*9840*	77.60	
	11		*9150*	72.16	

When selecting consumer caloric center 7 as a hydraulic end point, the volumetric flow is $\dot{V}_0 = 0.0044 \frac{m^3}{h}$.

The figures of volumetric flows, resistance factors, and differential pressures developed along each section are included in Table 4. The correlations used correspond to those described earlier.

Calculated constants are as follows in this case:

$A = 36779.8$,

$B = 0.4998$,

$C = 4.903$,

$A^* = 9490.96$,

$B^* = 0.0877$,

$C^* = 1.2923$.

Table 4 Hydraulic data of each section

	$\dot{V}$	v	Re	k/D	λ	R	Δp
	m^3/s	m/s	-	-	-	$bar \cdot s^2/m6$	bar
B	0.0612	1.949	956645	0.0008	0.01872	463.44	1.738
C	0.0484	2.740	1008581	0.0010	0.01994	1127.69	2.644
D	0.0287	1.624	597896	0.0010	0.02014	400.32	0.330
E	0.0159	0.899	330951	0.0010	0.02052	1181.45	0.298
F	0.0041	0.337	103502	0.0012	0.02276	893.60	0.015
G	0.0005	0.105	20549	0.0019	0.02944	32713.31	0.009
H	0.0038	0.762	149500	0.0019	0.02424	6445.88	0.094
I	0.0074	0.948	232539	0.0015	0.02266	2820.91	0.156
J	0.0132	0.420	206107	0.0008	0.01995	163.04	0.028
K	0.0940	1.916	1175170	0.0006	0.01778	22.95	0.203
L	0.1692	3.447	2114611	0.0006	0.01762	33.69	0.964
M	0.1760	3.586	2199828	0.0006	0.01761	4.49	0.139
1	0.0068	0.868	213043	0.0015	0.02274	5732.38	0.267
2	0.0128	1.632	400418	0.0015	0.02228	13696.75	2.249
3	0.0197	1.607	492822	0.0012	0.02107	193.39	0.075
4	0.0128	1.632	400418	0.0015	0.02228	866.88	0.142
5	0.0117	2.337	458812	0.0019	0.02344	13914.12	1.920
6	0.0036	1.089	173751	0.0023	0.02525	7113.44	0.093
7	0.0044	1.312	209291	0.0023	0.02510	15826.33	0.300
8	0.0036	1.089	173751	0.0023	0.02525	6435.97	0.084
9	0.0058	1.733	276422	0.0023	0.02492	36773.12	1.216
10	0.0808					370.50	2.421
11	0.0752					254.16	1.436

On the basis thereof, the value of k can be calculated.

$k = 0.1208$

In case of other nodes, figures lower than 0 or higher than 1 are yielded for k on the basis of this calculation principle as well, therefore only consumer 7 can be the hydraulic end point. Table 5 contains the values of k in case of different presumed hydraulic end points.

Table 5 Values of k

Hydraulic end point	Value of *k*
Consumer 4	2.192
Consumer 5	1.326
Consumer 6	1.080
Consumer 7	0.121
Consumer 8	-1.120

As regards the calculation principle, it is allowable to infringe Kirchhoff Laws, meaning that the aggregate figures of differential pressures calculated in the two directions are not required to be identical.

Figures of design pressure at each node as well as pump feed differential pressure are included in Table 6.

Table 6 Pressure values at each node and feed point

	Δp bar		Δp bar
VI.	0.3000	VI.	0.3000
V.	0.3091	VII.	0.3945
IV.	1.9202	VIII.	1.2160
III.	2.2184	IX.	2.4210
II.	2.5482	X.	2.6239
I.	5.1920	XI.	3.5884
SZ1	6.9298	SZ2	3.7275

When minimizing energy input, the two delivery head values do not agree: in this case, there are two different pumps. The operating points established are as follows:

$\Delta p_{SZ1} = 6.9298 bar,$

$\dot{V}_{SZ1} = \dot{V}_B = 0.0612 \frac{m^3}{s},$

$\Delta p_{SZ2} = 3.7275 bar$,
$\dot{V}_{SZ2} = \dot{V}_M = 0.1760 \frac{m^3}{s}$.

On the basis thereof, the power absorbed by each pump can be determined. Thus, the total power absorbed will be:
$P_{SZ1} = p_{SZ1} \cdot \dot{V}_{SZ1} = 6.9298 \cdot 0.0612 = 0.4243 bar \frac{m^3}{s} = 42.43 kW$,
$P_{SZ2} = p_{SZ2} \cdot \dot{V}_{SZ2} = 3.7275 \cdot 0.1760 = 0.6561 bar \frac{m^3}{s} = 65.61 kW$,
$P_{total} = P_{SZ1} + P_{SZ2} = 42.43 + 65.61 = 108.04 kW$.

By breaking up the loop at the pump, the network was converted into a two-feed radial network. In case of an appropriate design, after the correct selection of the hydraulic end point, the pressure pattern would be characterized by the fact that progressing along the mains, the pressure drop of the incoming consumer branch is always smaller at each node, meaning that damping is required on these branches. In this case, however, the design differential pressure at nodes IV, VIII and IX is the pressure drop of the consumer branch. Figure 7 illustrates the differential pressures available along the mains and their values required at critical nodes. The pressure pattern drawn on the mains had to be modified in accordance therewith, meaning that the feed differential pressure had to be increased. In addition to those listed above, critical nodes also include node x because a greater one would be necessary than what is available on the mains. It follows from this that the network was designed improperly. Pipe diameters are not large enough, therefore very high flow rates are produced. Consequently, pressure drops are too large on consumer branches.

In the diagram, light green lines indicate the differential pressures required at critical nodes. Thin red and blue lines show values available between the forward and return sections of the mains, while thick lines show the actual state established.

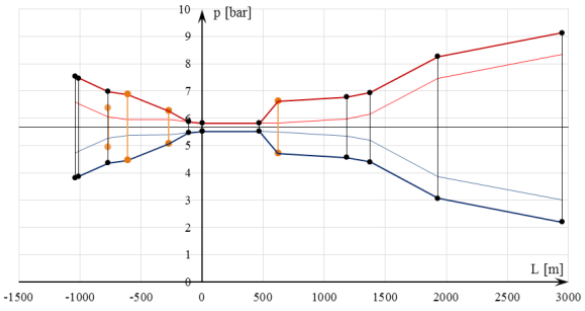

Fig. 7 Pressure conditions when work input is minimized

Figure 8 shows the actual pressure pattern, pressure drops at each consumer branch, and the damping required.

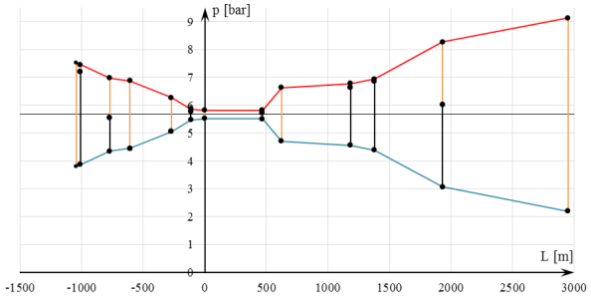

Fig. 8 Pressure pattern developed

The results yielded by the two calculation methods can be compared with the power absorbed by the pumps.
$P_{dissipated} = 132.67\ kW$,
$P_{input} = 108.04\ kW$.

Output reduction by the minimization of energy input can be calculated as compared to the one calculated for the minimum of dissipated energy.

$$\Delta P = \frac{P_{dissipated} - P_{input}}{P_{dissipated}} \cdot 100 = \frac{132.67 - 108.04}{132.67} \cdot 100 = 18.56\%.$$

It can be shown that a much more cost-effective operating state can be achieved by minimizing work input than by minimizing flow work. So it is worthwhile to break up the loop at the feed point and to apply two pumps instead of one. Obviously, these savings must be compared to the additional investment cost of the installation of two pumps.

4 Conclusion

Our study presented a hydraulic analysis method for district heating networks of a circular conduit system with given consumer volumetric flow demands, for both the dissipated energy minimum and the input energy minimum. After stating and arranging a loop equation and the node equations (Kirchhoff Laws I and II), the result is a quadratic equation for the distribution of consumer volumetric flow at the hydraulic end point. This is indicated by the so-called k factor, which is a figure lower than 1. Adoption of the procedure was presented in an example for each of the minimum of dissipated energy and pump work. By comparison of the results yielded, it was demonstrated that circular conduit operation by separated pumping is energetically more advantageous. Obviously, the issue to be examined is whether the installation of two pumping stations represents a better solution in respect of investment costs.

References

[1] Garbai, L. "*Távhőellátás*." (District heating.) Typotex Kiadó, 2012. (in Hungarian)

[2] Szanthó, Z., Németh, G. "The Role of Pipe-Diameters in Operating the Non-balanced Domestic Hot Water Circulation Systems." *WSEAS Transaction on Heat and Mass Transfer*. 1(6), pp. 660-665. 2006.

[3] Garbai, L., Barna, L., Szánthó, Z. "Hydraulic analysis of two-pipe central heating networks." *IASME Transactions*. 9(2), pp. 1809-1814. 2005.

[4] Halász, G., Kristóf, G., Kullmann, L. "Áramlások csőhálózatokban." (Flow in Pipeline systems.) Műegyetemi Kiadó, 2002. (in Hungarian)

[5] Dobersek, D., Goricanec, D., Krope, J. "Calibration of Pipe Networks for District Heating using the Non-linear Optimization Method. *International Journal of Nonlinear Sciences and Numerical Simulation*. 7(2), pp. 225–228, 2011.
https://doi.org/10.1515/IJNSNS.2006.7.2.225

[6] Dobersek, D., Goricanec, D. "Optimisation of tree path pipe network with nonlinear optimization method." *Applied Thermal Engineering*. 29(8–9), pp. 1584-1591. 2009.
https://doi.org/10.1016/j.applthermaleng.2008.07.017

[7] Dobersek, D., Goricanec, D., Krope, J. "Calibration of pipe networks for district heating using the nonlinear optimization method." *International Journal of Nonlinear Sciences and Numerical Simulation*. 7(2), pp. 225-228. 2006.
https://doi.org/10.1515/IJNSNS.2006.7.2.225

[8] Goricanec, D., Krope, J., Pristovnik, A. "Calculation of two-phase flow-pressure conditions and pipe systems." *International Journal of Nonlinear Sciences and Numerical Simulation*. 7(2), pp. 229-232. 2006.

[9] Guelpa, E., Toro, C., Sciacovelli, A., Melli, R., Sciubba, E., Verda, V. "Optimal operation of large district heating networks through fast fluid-dynamic simulation." *Energy*. 102, pp. 586-595. 2016.
https://doi.org/10.1016/j.energy.2016.02.058

[10] Sciacovelli, A., Guelpa, E., Verda, V. "Pumping cost minimization in an existing district heating network." In: ASME 2013 International Mechanical Engineering Congress and Exposition. San Diego, California, USA, Nov. 15-21, 2013.
https://doi.org/10.1115/IMECE2013-65169

[11] Ancona, M.A., Melino, F., Peretto, A. "An Optimization Procedure for District Heating Networks. *Energy Procedia*. 61, pp. 278-281. 2014.
https://doi.org/10.1016/j.egypro.2014.11.1107

[12] Teet-Andrus, K., Alo M., Ular, P. "The new dimensioning method of the district heating network." *Applied Thermal Engineering*. 71(1), pp. 78-82. 2014.
http://dx.doi.org/10.1016/j.applthermaleng.2014.05.087

[13] Wang, H., Yin, W., Zhou, Z., Lahdelma, R. "Optimizing the design of a district heating network." In: Proceedings of ECOS, 2015. Pau, France, June 30-July 3, 2015.